Journal of Catalysis 263 (2009) 306–314

Contents lists available at ScienceDirect

Journal of Catalysis

www.elsevier.com/locate/jcat

# Correlation of $H_2$ heat of adsorption and ethylene hydrogenation activity for supported Re@Pd overlayer catalysts

Michael P. Latusek, Brett P. Spigarelli, Rebecca M. Heimerl, Joseph H. Holles *

*Department of Chemical Engineering, Michigan Technological University, 1400 Townsend Drive, Houghton, MI 49931, United States*

ARTICLE INFO

*Article history:*
Received 12 December 2008
Revised 30 January 2009
Accepted 19 February 2009
Available online 13 March 2009

*Keywords:*
Ethylene hydrogenation
Hydrogen
Chemisorption
Overlayer catalysts
Pd
Re
Kinetics

ABSTRACT

Alumina-supported bimetallic overlayer Pd on Re (Re@Pd) catalysts were synthesized using the directed deposition technique. Hydrogen chemisorption, TEM, EDS, XRD, and ethylene hydrogenation studies were used to characterize the catalysts and provide indication of electronic modification of the Pd surface layer due to the overlayer particle structure. First principles computation and single crystal studies of Pd overlayers on Re in the literature have shown that electronic modification of the Pd overlayer is observed and leads to decreased binding strength for chemisorbed species such as $H_2$, $C_2H_4$, and CO. Measured hydrogen chemisorption isotherms indicated that Pd was deposited on the Re and not as pure isolated Pd particles. $H_2$ heats of adsorption, as determined by chemisorption, indicated that the Re@Pd overlayer catalysts were lower than either pure Pd or Re. The Re@Pd catalysts were slightly less active for ethylene hydrogenation than pure Pd but displayed similar apparent activation energies and $H_2$ and $C_2H_4$ reaction orders. A linear correlation between turnover frequency and maximum heat of $H_2$ adsorption was observed for the Pd and Re@Pd catalysts. This suggests an electronic modification of the Re@Pd catalyst surface compared to Pd as predicted in the literature by first principles computational studies.



## 1. Introduction

Bimetallic catalysts have long been an important area of catalysis research. Certain combinations of metals are known to improve activity, selectivity, or catalyst lifetime, such as Pt–Re for gasoline production through reforming [1]. Several mechanisms to explain the catalytic properties observed using bimetallic catalysts have been proposed, including structure effects [2], bifunctional routes [3], and electronic modification of surface properties [4].

Bimetallic overlayers, which consist of a monatomic metal layer deposited on a different bulk metal, have been frequently studied using single crystal and first principles computation techniques in an attempt to better understand the surface properties of bimetallic catalysts [5–12]. These overlayer systems have typically been found to possess very different surface properties compared to their component metals. The altered properties found in many overlayer systems have been explained by an electronic interaction that leads to a shift in the *d*-band center of an overlayer metal when it is deposited on a suitable base metal [13,14].

Overlayer systems have also been shown to exhibit distinctive reactivity properties compared to their pure components as well. Cyclohexene decomposition activity has been found to be lower in the Pt monolayer on W ($Pt_{ML}/W$) system compared to either Pt or W single crystal surfaces [15]. Pallassana and Neurock have studied the $Pd_{ML}/Re$ system using first principles computation for hydrogen and ethylene adsorption [16–18]. They found that the heats of hydrogen and ethylene adsorption are significantly lower on the monolayer system compared to pure Pd or Re. They also examined this system for ethylene hydrogenation and found that the activation barrier for ethylene hydrogenation changes very little for $Pd_{ML}/Re$ (78 kJ/mol) compared to pure Pd (82 kJ/mol). However, the activation barrier for the reverse reaction (dehydrogenation) increases significantly from 82 kJ/mol on Pd to 126 kJ/mol on $Pd_{ML}/Re$ [17]. These works suggest that the $Pd_{ML}/Re$ system may exhibit unique catalytic activity if a suitable technique for its synthesis as a supported bimetallic overlayer catalyst can be developed.

There are several synthesis methods mentioned in the literature which have been used to selectively deposit one metal onto a different base metal nanoparticle to obtain a core@shell structure. Some of these methods, such as polyol reduction, result in reduced, unsupported particles which then require impregnation onto a support in a later step [19]. Other methods are based on electroless deposition, which can lead to the undesirable formation of three-dimensional islands before complete monolayer deposition [20–23]. Thus there is still a need to develop methods to synthesize bimetallic overlayer catalysts directly on the support

* Corresponding author. Fax: +1 906 487 3213.
*E-mail address:* jhholles@mtu.edu (J.H. Holles).

0021-9517/$ – see front matter 
doi:10.1016/j.jcat.2009.02.022

that can exhibit properties consistent with first principles predictions.

In this work, high surface area supported Re@Pd (core@shell) overlayer catalysts were synthesized using the directed deposition technique. This technique is able to synthesize supported bimetallic overlayer catalysts by directing the deposition of overlayer metal onto pre-existing base metal particles using a surface reaction. The intent of this work is to examine the particle structure of supported Re@Pd catalysts, determine the effect of that structure using a probe reaction, relate the structure effects to synthesis conditions, and finally, compare these results to computationally predicted values. Based on the existing first principles computational research and the well-known use of ethylene hydrogenation as a probe reaction, it was decided to examine these new overlayer catalysts using ethylene hydrogenation [24].

## 2. Experimental

### 2.1. Catalyst synthesis

The monometallic catalysts studied in this paper were synthesized using standard techniques and were supported with 100 $m^2/g$ $\gamma$-alumina (Alfa Aesar, 99.97%). A 0.1 wt% $Pd/Al_2O_3$ control catalyst was prepared from a slurry of alumina and palladium (II) acetylacetonate (Alfa Aesar) in toluene. A large batch of 2 wt% $Re/Al_2O_3$ catalyst was used as a control and as a base for bimetallic catalyst synthesis. This catalyst was prepared by incipient wetness impregnation of alumina with a solution of ammonium perrhenate (Alfa Aesar, 99.999%). Catalysts were dried in a oven for several hours after synthesis, then calcined in air at 400 °C for 4 h using a 3 °C/min ramp rate. Finally, the catalysts were reduced in a 60 sccm $H_2$ flow for 2–4 h using a 3 °C/min ramp rate. The $Pd/Al_2O_3$ catalyst was reduced at 400 °C, while literature reports suggested rhenium required a temperature of 550 °C to be thoroughly reduced [25,26].

The supported overlayer catalysts described in this paper were synthesized using the directed deposition technique. This technique was adapted from the refilling technique used for controlling particle size in $Pt/Al_2O_3$ catalysts as described by Womes et al. [27]. The synthesis procedure was started by reducing the previously synthesized base $Re/Al_2O_3$ catalyst as described above for the monometallic catalyst. In order to inhibit overlayer metal precursor adsorption by the support (to prevent formation of new particles), water-saturated helium gas was then passed over the catalyst at room temperature for 24 h. The desired Pd overlayer is deposited onto the Re base via a hydrogenation reaction that decomposes the palladium (II) acetylacetonate precursor:

$$Pd(acac)_2 + 2 \cdot Re - H \rightarrow 2 \cdot Re - Pd + 2 \cdot acacH.$$

Based on this reaction, adsorbed $H_2$ on the base Re particles is necessary to achieve the overlayer deposition. A final treatment in flowing $H_2$ was performed for 1 h at 100 °C after the previous support passivation procedure to provide the source of adsorbed hydrogen. The 100 °C treatment temperature corresponds to the temperature of maximum irreversible $H_2$ adsorption by the Re base metal, which was determined from $H_2$ chemisorption experiments.

To ensure support adsorption of the overlayer metal precursor is as low as possible, acetylacetone was also used as an inhibitor. This was achieved by transferring the catalyst to a beaker of toluene and acetylacetone (Sigma-Aldrich, 99+%) after the $H_2$ treatment. After 15 min a solution of toluene and Pd (II) acetylacetonate was added to begin the overlayer deposition reaction. The reaction was maintained at 60 °C, with the volatile reactor contents maintained in the flask using a water-cooled condenser. After two hours, the catalysts were filtered and washed with fresh toluene. Finally, the catalysts were dried in an oven, calcined in air at 400 °C for 4 h, and reduced in 60 sccm $H_2$ at 400 °C for 4 h.

**Table 1**
Catalyst metal loadings from elemental analysis.

| Catalyst | Re (wt%) | Pd (wt% ) |
|---|---|---|
| Re | 1.26 | – |
| Re@Pd HT | 1.26 | 0.083 |
| Re@Pd TD | 1.26 | 0.073 |
| Re@Pd NI | 1.26 | 0.249 |
| Pd | – | 0.086 |

Three different Re@Pd overlayer catalysts were synthesized using the above technique modified in different ways. One catalyst was synthesized exactly as described above (Re@Pd HT for high temperature deposition of Pd). A second was performed also as described above, but the complete synthesis procedure was repeated on the same catalyst a total of three times (Re@Pd TD for triple deposition). The last catalyst was performed without the water-saturated helium and acetylacetone inhibition procedures (Re@Pd NI for no inhibitor). This catalyst was expected to have Pd deposition as an overlayer on Re particles, as well as on the alumina support forming monometallic particles. Because all of the Re@Pd catalysts were synthesized with the same Re base catalyst, direct comparisons of particle size/structure between all the catalysts are possible. The maximum expected palladium content for each Re@Pd catalyst is 0.27 wt%, based on the amount added during palladium deposition.

### 2.2. Sample characterization

Elemental analysis by Galbraith Laboratories, Inc. was used to determine metal loadings for all catalysts synthesized in this study. These loadings are reported in Table 1.

Chemisorption experiments were performed using a Micromeritics ASAP 2020 instrument. Samples were prepared for each analysis by reduction at 400 °C in flowing $H_2$. Isotherms were typically obtained at temperatures ranging from 35 °C to 400 °C and pressures of 1 mTorr to 800 Torr. Reversible adsorption isotherms were obtained after a 30 min evacuation at the experiment temperature following completion of the total adsorption isotherm. A leak rate of less than 2 mTorr/min was maintained for accuracy in the low pressure region of the isotherms.

Reactivity experiments using the ethylene hydrogenation reaction were performed in a 6 mm diameter tubular glass reactor. The reactor was outfitted with an ethylene glycol/water cooling jacket that enabled precise temperature control between −10 °C and 70 °C. Typical temperatures were −10 °C to 30 °C. Reaction order determination experiments were performed at 10 °C. Catalyst samples (typically ∼25 mg) were sieved to −100 mesh and diluted in 350 mg silica gel (Alfa Aesar, 70–150 mesh) before being loaded into the glass reactor. Quartz wool was used to hold the catalyst powder in place. Ethylene (99.9%) and hydrogen (99.999%) were obtained from Praxair. Nitrogen (Linde) was used as the inert make-up gas.

Mass flow controllers (FMA-700 Series from Omega) were used to control gas flow rates. Total flow rates of 100–1500 mL/min were possible with this setup, with 750 mL/min being the standard flow rate for reactivity experiments. Ethylene concentrations between 0.35 vol% and 10 vol% were used during ethylene reaction order determination experiments, with 3 vol% ethylene being standard. Hydrogen concentrations between 10 vol% and 50 vol% were used during hydrogen reaction order determination experiments, with 20 vol% hydrogen being standard. At the standard conditions, reactor pressure was approximately 3 psig. Reactor effluent was analyzed by GC/MS (Thermo-Finnigan Trace GC/Trace DSQ) using a

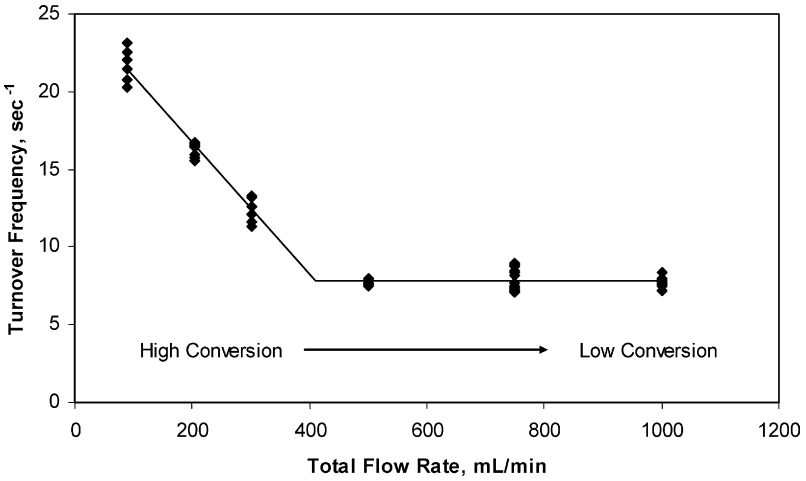


**Fig. 1.** Measured turnover frequency as a function of total flow rate at 303 K.

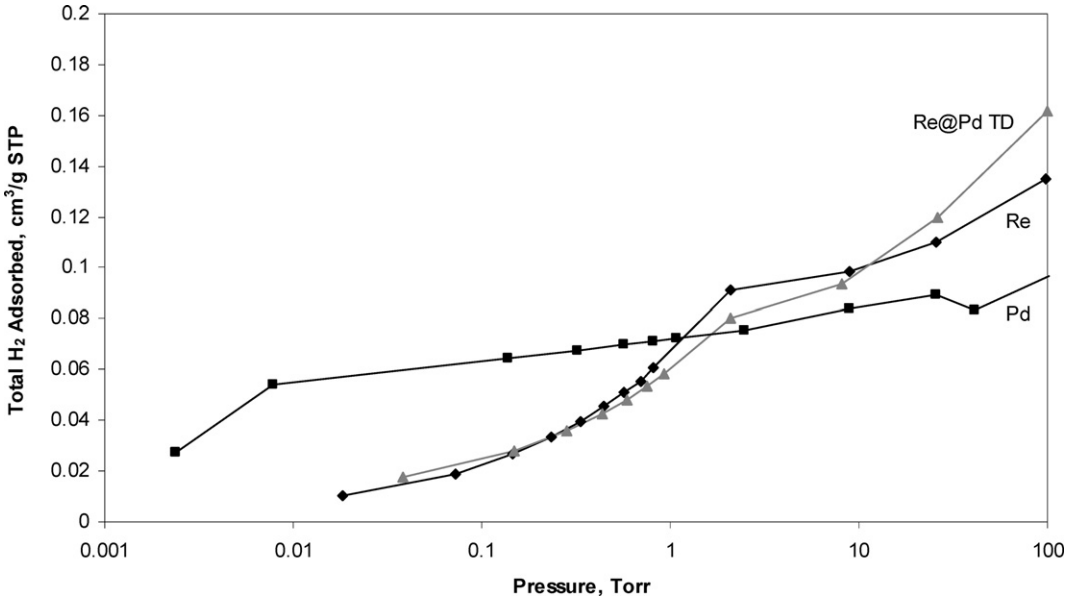


**Fig. 2.** Log-scale isotherms for Re, Pd, and Re@Pd TD catalysts at 50 °C.

6-port gas sampling valve. A 10 m Varian PLOT column was used for chromatographic separation of ethane and ethylene.

Transport limitation experiments were carried out to determine the proper conditions for performing reactivity experiments. The transport limitation experiments were performed by measuring turnover frequency at constant temperature and inlet concentrations, but varying total flow rates. The results of one of these experiments performed at 303 K are shown in Fig. 1. The measured turnover frequency, which is independent of total flow rate when transport limitations are absent, was observed to increase below 500 mL/min total flow rate. This flow rate corresponded to approximately 2% conversion of ethylene, therefore indicating that conversion should be maintained below 2% in order to prevent heat transfer limitations from this fast and exothermic reaction from impacting reactivity results. Typical conversions for the results presented in this paper were 0.03–1.5%.

Transmission election microscopy (TEM) and energy dispersive X-ray spectroscopy (EDS) was performed on a JEOL JEM-4000FX microscope operating at 200 kV. Carbon-coated nylon grids (SPI Supplies) were used to reduce the copper background spectrum, which was found to interfere with analysis of rhenium during EDS measurements.

## 3. Results and discussion

### 3.1. Hydrogen chemisorption

Hydrogen chemisorption isotherms at 50 °C for the Pd, Re and Re@Pd TD catalysts are shown in Fig. 2. The isotherms include both reversible and irreversible adsorption and reveal important adsorption characteristics for each catalyst. The pure Pd catalyst shows that most low pressure adsorption occurs below 0.01 Torr, while the pure Re catalyst shows that most low pressure adsorption occurs between 0.1–2 Torr. Although the Re@Pd TD catalyst contains a similar amount of Pd as the pure Pd catalyst (see Table 1 for metal loadings), the isotherm from the Re@Pd TD catalyst does not show a linear combination of the two pure metal isotherms. Rather, this isotherm maintains the isotherm features and adsorption quantities of the pure Re catalyst. The isotherm for the overlayer catalyst thus indicates that no particles of pure Pd were formed during the synthesis process and that Pd was primarily deposited on existing Re sites active for $H_2$ chemisorption. Although not shown here, the isotherm for the Re@Pd HT catalyst was very similar to that of Re@Pd TD. The isotherm for Re@Pd NI demonstrated significant $H_2$ uptake below 0.01 Torr as in the

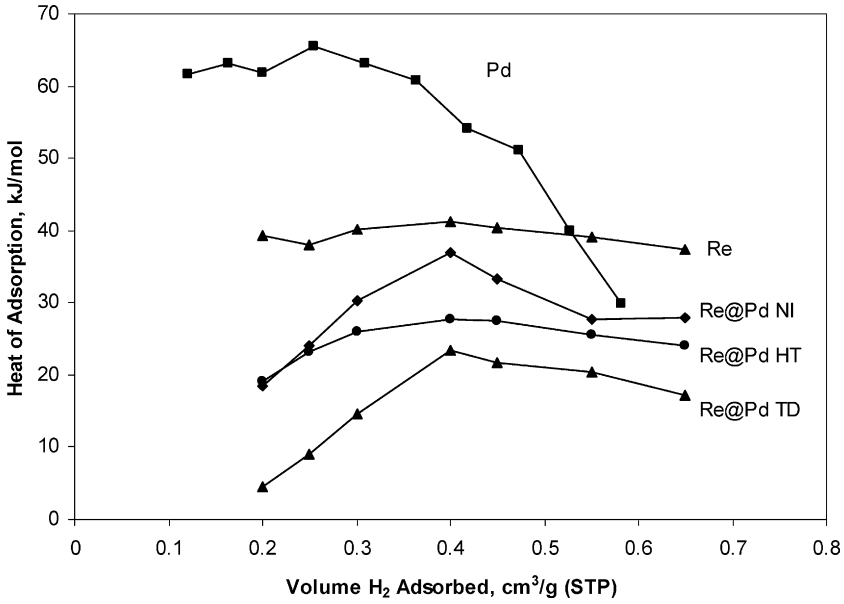


**Fig. 3.** Isosteric heat of $H_2$ adsorption on all studied catalysts as a function of volume adsorbed.

pure Pd catalyst, along with adsorption between 0.1–2 Torr. The low pressure uptake in this catalyst suggests formation of pure Pd particles, which is consistent with the synthesis procedure for this catalyst which did not utilize inhibitors to prevent formation of monometallic Pd particles on the support.

The heat of hydrogen adsorption for each catalyst was calculated from isotherms obtained at multiple temperatures using the Clausius–Clapeyron equation, the use of which has been well documented in the literature [28–30]. Resulting values for heat of adsorption as a function of the quantity of adsorbed hydrogen are presented in Fig. 3. Results for heat of adsorption on Pd of approximately 60 kJ/mol at low coverage compare well with literature results. Chou et al. measure a value of 67 kJ/mol for hydrogen adsorption on highly dispersed $Pd/Al_2O_3$ [30], while the value from first principles computation for single crystal Pd(111) was determined to be 78 kJ/mol at 100% coverage of fcc sites [17]. Re heats of adsorption were fairly constant at approximately 40 kJ/mol for all coverages examined. No values for heat of hydrogen adsorption on Re at high coverage have been found in the literature, but initial (i.e., low coverage) heats have been reported to be in the range of 128–139 kJ/mol for unsupported rhenium [18,31].

The Re@Pd catalysts all show decreased adsorption heats compared to the pure Pd catalyst and the base Re catalyst from which they were synthesized from, in agreement with theoretical predictions. The maximum values calculated for each catalyst were 37, 28, and 23 kJ/mol for the Re@Pd NI, HT, and TD catalysts, respectively. The heat of adsorption on the Re@Pd NI catalyst is higher than the other Re@Pd catalysts, which may be due to the presence of isolated Pd particles as indicated by chemisorption isotherms. At 100% coverage of fcc sites, Pallassana and Neurock predicted the hydrogen heat of adsorption to decrease from an exothermic −78 kJ/mol to an endothermic +2 kJ/mol on Pd(111) and $Pd_{ML}/Re(0001)$, respectively [17]. Similarly, we observe that hydrogen heat of adsorption decreases from 63 kJ/mol on Pd to 15 kJ/mol on Re@Pd TD at 0.3 $cm^3/g$ (STP) hydrogen coverage. The significantly decreased heats of adsorption shown in Fig. 3 are consistent with the formation of a Pd overlayer on Re particles as desired. The different metal loadings and synthesis methods also yield a range of maximum adsorption heats which, together with ethylene hydrogenation activity, may be used to determine structure/property relationships for the catalysts.

### 3.2. TEM/EDS results

TEM imaging was unable to observe metal particles on any of the synthesized catalysts, suggesting that the deposited metals are highly dispersed on the alumina surface. Rhenium is known to form highly dispersed phases on alumina even at 1 wt% concentrations, making it generally difficult to observe particles with TEM [32]. No particle observation for the Re@Pd catalysts also indicates that palladium has been deposited on rhenium particles as desired or as a highly dispersed phase.

Since metal particles could not be observed directly, EDS was also performed to look for regions on the alumina particles where Pd or Re peak intensities were higher or lower than the average intensity for the entire particle. No Pd peaks were observed on any of the Re@Pd catalysts, likely owing to the very low loading of Pd on these catalysts. In contrast, Re peaks were observed on all of the Re@Pd catalysts, but its intensity was approximately constant regardless of the location or diameter of the electron beam on an alumina particle. Fig. 4 shows the results from a sample EDS experiment on the Re@Pd TD catalyst, where the electron beam was first spread over an entire alumina particle (wide beam area), then condensed to illuminate a small region of the same particle (condensed beam area). The resultant rhenium peaks for these very different sized areas was little changed, suggesting a uniform distribution of very small Re particles on the alumina surface.

Estimated Re dispersion determined from chemisorption at 100 °C was 34.6%, which gives an average particle size of 3.9 nm assuming spherical particles, the Re atomic cross-sectional area is 0.065 $nm^2$, and the Re density is 21.04 $g/cm^3$ [33]. This particle size may be large enough to observe using TEM if the dispersion is accurately reflected by hydrogen chemisorption. However, the data of Chadzynski and Kubicka show that the conditions of $H_2$ isotherm measurement can significantly affect dispersion estimates. Under similar analysis conditions as those of this work, their results showed that irreversible $H_2$ adsorption for a 1 wt% $Re/Al_2O_3$ catalyst at 100–200 °C produced a dispersion of only approximately 40%, while the dispersion determined under other conditions and by TEM was 90% [33]. Their results suggest that the true particle dispersion for the Re and Re@Pd catalysts is likely much larger than the 34.6% value determined from chemisorption, decreasing the estimated particle size enough that detection by TEM may be expected to be very difficult.

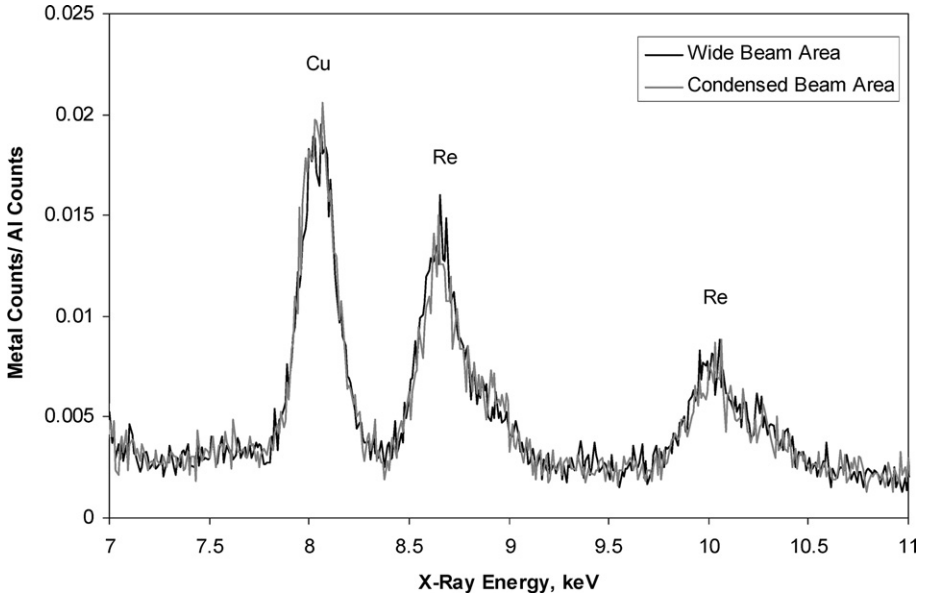


**Fig. 4.** Recorded EDS spectra for Re@Pd TD catalyst showing normalized metal counts as a function of energy.

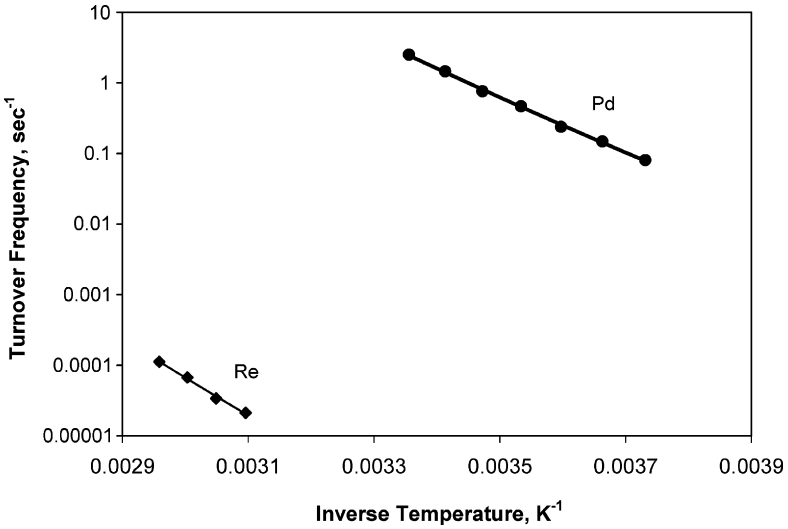


**Fig. 5.** Re and Pd catalyst Arrhenius-type plot for ethylene hydrogenation (3% ethylene, 20% hydrogen, balance nitrogen).

Diffraction patterns were also obtained for the Re@Pd NI catalyst on the TEM with the electron beam expanded over an entire alumina particle. Prior to obtaining the diffraction patterns, the alumina particles were verified by EDS to contain rhenium. The diffraction patterns for this catalyst were compared against diffraction patterns obtained from a sample of the pure $\gamma$-alumina support. Both samples displayed ring-diffraction patterns. Imaging software was used to measure the radius of each displayed ring pattern. These values were indexed against the expected atomic spacings for $\gamma$-alumina, rhenium, and palladium. Three diffraction patterns were obtained on different Re@Pd NI particles. All of the rings observed coincided with the expected atomic spacings for alumina except in one case, where a single ring was observed that was found to closely match the 1.1948 Å rhenium *d*-spacing. This finding, along with the lack of observed Re diffraction rings in the other patterns, simply highlights the low concentrations of metals on the alumina support for these catalysts, while also suggesting the presence of very small rhenium particles due to the observed ring pattern for rhenium.

### 3.3. Ethylene hydrogenation results

Arrhenius-type plots for $Pd/Al_2O_3$ and $Re/Al_2O_3$ catalysts are shown in Fig. 5 for the ethylene hydrogenation reaction. Reaction rates on palladium are several orders of magnitude higher than on rhenium. The Arrhenius-type plots for Pd and Re@Pd catalysts shown in Fig. 6 indicate that Re@Pd catalysts have activities for the ethylene hydrogenation reaction very similar to pure Pd catalysts. Due to the much higher activity of bimetallic Re@Pd catalysts compared to Re, it stands to reason that this reactivity can be attributed entirely to the presence of palladium. For this reason, turnover frequencies for all palladium-containing catalysts were calculated based on measured palladium content from elemental analysis (see Table 1 for metal loadings). Dispersion values used in turnover frequency calculations were 0.5 for the Pure Pd catalyst (determined from $H_2$ chemisorption at 35 °C) and unity for all Re@Pd catalysts.

The Arrhenius-type plots of Fig. 6 graphically indicate the relative reaction rates and apparent activation energies for the palladium-containing catalysts. Table 2 lists the calculated acti-

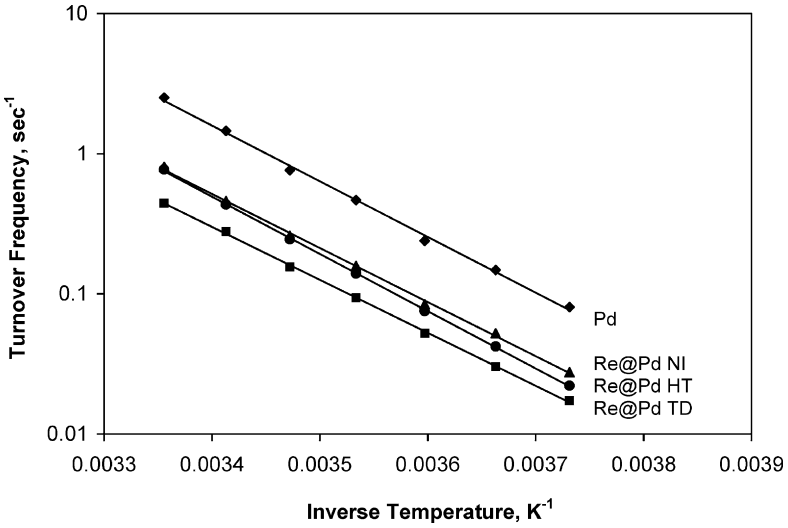


**Fig. 6.** Pd and Re@Pd catalyst Arrhenius-type plot for ethylene hydrogenation (3% ethylene, 20% hydrogen, balance nitrogen).

**Table 2**
Measured catalyst activation energies and reaction orders.

| Catalyst | Apparent activation energy, kJ/mol | Reaction order | |
|---|---|---|---|
| | | $H_2$ | $C_2H_4$ |
| 10 wt% $Re/Al_2O_3$ | $103 \pm 23$ | 1.0 | −0.01 |
| 0.1 wt% $Pd/Al_2O_3$ | $76.1 \pm 4.2$ | 1.0 | −0.11 |
| Re@Pd HT | $78.3 \pm 1.5$ | 1.1 | −0.12 |
| Re@Pd TD | $72.4 \pm 1.9$ | 1.0 | −0.12 |
| Re@Pd NI | $73.9 \pm 3.0$ | 1.0 | −0.12 |

vation energies and associated uncertainties based on Fig. 6. The Re@Pd catalysts show only small differences in reaction rates and apparent activation energies. Based on the uncertainties, some of the activation energies are indistinguishable, while others are distinct. Regardless, with the exception of Re, they are all very similar and indicate that the overlayer catalyst structure has not resulted in a mechanism change. The pure Pd catalyst shows an activation energy in the same range as the Re@Pd catalysts but approximately 3 times larger reaction rates. The Re@Pd NI catalyst exhibits higher activity more similar to the pure Pd catalyst than the other two Re@Pd catalysts. This may be due to the presence of a small amount of isolated Pd as indicated by the chemisorption isotherms.

Apparent activation energies for ethylene hydrogenation on palladium have been widely reported in the literature to be between 21 and 50 kJ/mol, while the activation energies measured here are approximately 75 kJ/mol [34]. The reason for this discrepancy is not immediately apparent considering the great lengths gone to eliminating heat and mass transfer effects during measurements. No activation energy values for ethylene hydrogenation on rhenium were found in the literature, likely owing to its poor activity for this reaction.

Hydrogen and ethylene reaction orders were determined by holding the flow rate of one reactant constant while varying the other and adjusting the nitrogen flow rate to maintain constant total flow rate. Reaction order plots for hydrogen and ethylene can be found in Figs. 7 and 8, with resulting values listed in Table 2. All catalysts were found to show a first order dependence on hydrogen and a slightly negative order in ethylene. At ethylene concentrations above ~10%, the reaction rate is independent (zero order) of ethylene concentration. Similar reaction orders were determined for ethylene hydrogenation studies on Pd using first-principles based Monte Carlo simulations [35].

Goddard et al. have shown previously that ethylene hydrogenation on platinum proceeds via a modified Horiuti–Polanyi mechanism which contains both competitive and noncompetitive hydrogen adsorption sites [36,37]. No similar experimental mechanism studies were found for Pd. The modified Horiuti–Polanyi mechanism is listed below [36,37]:

1. $H_2 + 2S \leftrightarrow 2HS$;
2. $HS + S' \leftrightarrow HS' + S$;
3. $H_2 + 2^* \leftrightarrow 2H^*$;
4. $H^* + S' \leftrightarrow HS' + *$;
5. $C_2H_4 + 2^* \leftrightarrow {}^*C_2H_4{}^*$;
6. ${}^*C_2H_4{}^* + HS' \leftrightarrow {}^*C_2H_5{}^* + S'$;
7. ${}^*C_2H_5{}^* + HS' \leftrightarrow C_2H_6 + 2^* + S'$.

The S sites are noncompetitive hydrogen adsorption sites that are inaccessible for ethylene adsorption (explained by the small size of hydrogen), while the * sites are competitive sites that are accessible to both hydrogen and ethylene. Goddard et al. included hydrogen activation steps (S′ sites) to explain isotopic product distribution observations [36]. They also determined that the ethylene order was zero above 75 Torr ethylene pressures and slightly negative at lower pressures, similar to the observations from Fig. 8 here [36,37]. Hansen and Neurock also demonstrated using Monte Carlo simulations that Pd reaction orders similar to those reported here would result if lateral interactions were included, thus not requiring separate ethylene and hydrogen adsorption sites [35]. A hydrogen order that shifted from 0.5 at 248 K to unity at 336 K was also noted [36,37]. Based on the similar reaction order results, it appears that the ethylene hydrogenation mechanisms previously shown in the literature also apply to the Pd, Re, and Re@Pd catalysts synthesized for this work. There is no indication that the deposition of Pd on Re has resulted in a mechanism change.

Aside from the Re@Pd NI catalyst, chemisorption isotherms indicate that palladium content in the Re@Pd catalysts is not present in significant amounts as isolated Pd particles, instead forming bimetallic particles that present adsorption behavior similar to rhenium. While it is possible that Re may re-segregate to the surface as an oxide during the calcination step of the synthesis procedure, the sample was subsequently reduced in $H_2$. Christoffersen et al. have shown that when metallic Pd and Re are present together, Pd will show a strong surface segregation [14]. In addition, turnover frequencies, which were calculated based on Pd content alone, are comparable across all of the Pd and Re@Pd catalysts.

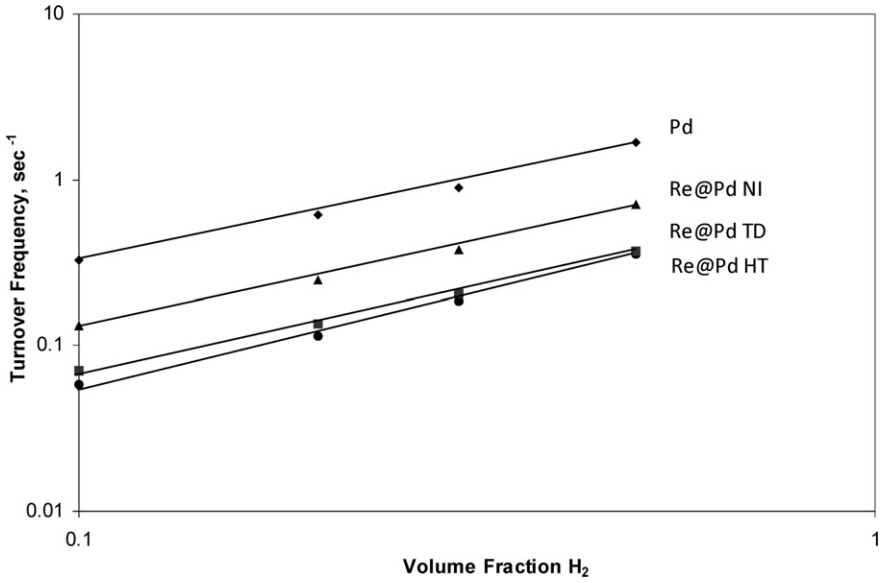


**Fig. 7.** Hydrogen reaction order plot for ethylene hydrogenation (3% ethylene, 10–50% hydrogen, balance nitrogen).

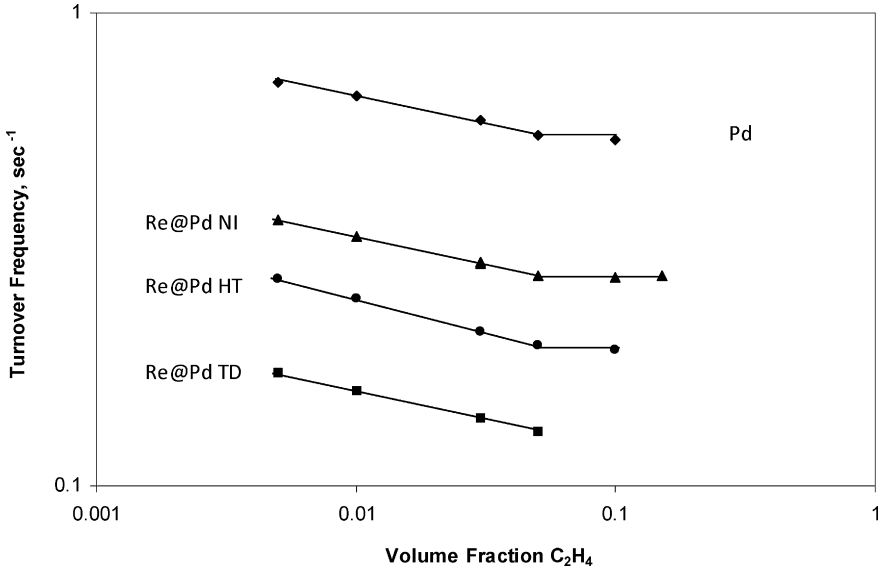


**Fig. 8.** Ethylene reaction order plot for ethylene hydrogenation (0.5–15% ethylene, 20% hydrogen, balance nitrogen).

These results suggest the existence of a palladium/rhenium interaction consistent with a Pd overlayer deposited on rhenium for the Re@Pd catalysts. Heat of adsorption values calculated from hydrogen chemisorption isotherms also indicate that the Re@Pd catalysts bind hydrogen more weakly than rhenium or palladium, in agreement with single crystal and first principles computational studies. While these results suggest that the directed deposition synthesis technique has been successfully used to create the desired overlayer catalysts, there is an apparent discrepancy between the observed reactivity and hydrogen adsorption properties. Chemisorption results suggest that hydrogen adsorption behavior on Re@Pd catalysts is similar to rhenium, but with notably weaker binding strength. In contrast, reactivity results suggest that the Re@Pd surface is little changed from pure Pd except for a slightly decreased activity.

The slightly decreased activity can be explained by considering the reaction mechanism and the consequences of decreased hydrogen heat of adsorption. Because ethylene hydrogenation is first order in hydrogen and slightly negative in ethylene, the reaction rate is dependent on the hydrogen surface coverage, which depends on the rates of hydrogen adsorption and desorption, as well as the rate of reaction. A decrease in hydrogen adsorption strength will increase the desorption rate, decreasing surface coverage and hence decreasing the overall reaction rate as was observed. This correlation between hydrogen adsorption strength and reaction rate can be seen in Fig. 9, which plots the maximum heat of hydrogen adsorption determined from the chemisorption results against the turnover frequency measured for each palladium-containing catalyst at 273 K. The apparent relationship from this data set is consistent with the suggestion that ethylene hydrogenation on a palladium surface at the conditions of this work is affected by the availability of adsorbed hydrogen.

Direct literature reactivity comparisons with this work are difficult. Most of the literature studies have examined only hydrogen and alkene (ethylene, 1-butene, 1-hexene, and cyclohexene) temperature programmed desorption (TPD) or temperature programmed reaction (TPR) of an alkene with a predosed hydrogen surface (see Chen et al. for a summary [38]). The TPD studies show hydrogen and alkenes are less strongly bound as the *d*-band center moves further away from the Fermi level. This is in agreement

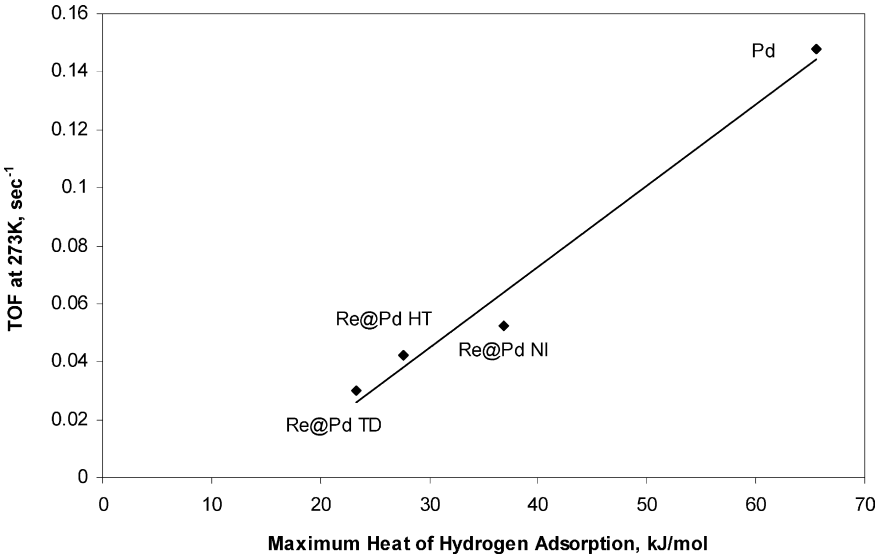


**Fig. 9.** Correlation between hydrogen heat of adsorption and ethylene hydrogenation turnover frequency for studied Re@Pd and Pd catalysts.

with our hydrogen studies. Perhaps the best comparison of these studies with ours is the work by Humbert and Chen involving hydrogen and cyclohexene [39]. They developed a plot showing TPR hydrogenation activity first increasing and then decreasing as the cyclohexene binding energy decreased (or as the center of the *d*-band moved closer to the Fermi level). Thus depending on the situation, hydrogenation activity can indeed decrease as the hydrogen binding energy decreases. The high initial hydrogen coverages resulting from the predosing by Humbert and Chen may also parallel the possible reaction conditions where the hydrogen partial pressure is increased to increase the hydrogen surface coverage. The situation of higher coverage and weaker hydrogen bonding may then result in an activity increase for the overlayer catalysts compared to pure Pd.

If the activation barriers for hydrogenation were also affected by the overlayer structure, significant changes in reaction rate or reaction orders may be possible. First principles computation of ethylene hydrogenation on $Pd_{ML}/Re$ and Pd instead indicate that the forward activation barrier for ethylene hydrogenation to surface ethyl ($C_2H_5$) is relatively unchanged (78 kJ/mol on $Pd_{ML}/Re$ vs 82 kJ/mol on Pd) [17]. These values compare very well with the apparent activation energies obtained on the Pd and Re@Pd catalysts studied here (72.4–78.3 kJ/mol). The agreement of our measured values with the calculated values from the literature leaves open the possibility that the apparent activation energy measured here is the activation barrier for hydrogenation of adsorbed ethylene to ethyl. This is possible since a first order hydrogen dependence does not automatically imply that the reaction rate is limited by hydrogen adsorption. A first order hydrogen dependence is equally possible when the surface reaction is limiting, but hydrogen coverage is low compared to ethylene as suggested in this case by the slightly negative ethylene order that was observed. Only the reverse activation barrier was projected by computational studies to be altered significantly (126 kJ/mol on $Pd_{ML}/Re$ vs 82 kJ/mol on Pd), but the effect of this would only be observable under conditions where the reaction is reversible. Therefore, the measured values for activation energy and reaction orders are consistent with the predicted activation barriers for the reaction at the conditions of this work.

The correlation observed in Fig. 9 suggests that ethylene hydrogenation activity could be increased through electronic modification of a Pd overlayer that results in stronger $H_2$ adsorption. First principles computation research has shown that a decrease in the *d*-band center of a metal surface will result in lower adsorbate binding strengths, while an increase in the *d*-band center results in stronger binding of adsorbates [13,14,17]. Christoffersen et al. used first principles computational techniques to predict the *d*-band shifts for a number of bimetallic overlayer systems. In order to achieve stronger adsorbate binding on a Pd overlayer, their results point to the $Pd_{ML}/Ag$ and $Pd_{ML}/Au$ systems as capable of providing this desired property [14]. However, their data also suggests that Ag and Au will tend to surface segregate or alloy with Pd, making the Pd overlayers on Ag and Au unstable for synthesis and characterization efforts [14,40]. Single crystal work has also indicated Au segregation or alloying in the Pd/Au system [8,41]. Finally, increasing metal–hydrogen bond strength too much may not always be beneficial either. If the hydrogen is too strongly bound, this can also limit reactivity. If the bond becomes too strong, the resulting decrease in activity might manifest itself in a volcano plot similar to that of Humbert and Chen [39].

Christoffersen et al. have also shown a linear relationship between calculated $H_2$ adsorption energy and *d*-band center for a number of transition metals and pseudomorphic overlayers (such as $Pt_{ML}/Ru$ and $Pd_{ML}/Re$) [14]. Our results above have further demonstrated a correlation between $H_2$ heats of adsorption and ethylene hydrogenation activity. Thus, for ethylene hydrogenation and the Re and Pd system, there appears to be a direct relationship between activity and the calculated center of the *d*-band.

Research by Zhou et al. with Cu@Pt catalysts supported on alumina for NO reduction showed that the Cu@Pt catalysts had equal activity as pure Pt catalysts. However, they also found a significantly increased selectivity for $N_2$ formation on the Cu@Pt catalyst compared to pure Pt [42]. This result, along with the results presented here, indicates that it may be possible that overlayer catalysts will in general provide similar activities as catalysts consisting of the pure overlayer metal, but with differing selectivity.

## 4. Conclusions

Hydrogen chemisorption and ethylene hydrogenation results both suggest the formation of Pd overlayers on Re for the catalysts studied here. Chemisorption isotherms and hydrogen heats of adsorption show distinctly different hydrogen adsorption behavior than would be expected for a physical mixture of Pd and Re particles and are in agreement with previous literature first principles computation and single crystal studies of $Pd_{ML}/Re$ [16–18]. Ethylene hydrogenation results suggest a highly dispersed Pd surface layer that displays similar reactivity properties as pure Pd, however, the Re@Pd catalysts show decreased TOF compared to

pure Pd. A correlation between measured hydrogen heat of adsorption and TOF was also observed for Pd-containing catalysts.

All of these results are consistent with electronic modification of Pd by the formation of Pd overlayers on Re, which was the desired outcome from the use of the directed deposition synthesis technique. Ethylene hydrogenation activity was observed to be mildly inhibited for this particular overlayer system due to the decrease in surface hydrogen, which suggests that activity enhancement may be observed if a Pd overlayer system was developed that could bind hydrogen more strongly than pure Pd.

## Acknowledgments

The authors gratefully acknowledge funding support from the Center for Fundamental and Applied Research in Nanostructured and Lightweight Materials at Michigan Technological University sponsored by the National Renewable Energy Laboratory of the Department of Energy through grant number DE-FG36-08GO88104.

## References

[1] J.P.M. Treichel, in: J.I. Kroschwitz, M. Howe-Grant (Eds.), Kirk-Othmer Encyclopedia of Chemical Technology, vol. 21, John Wiley & Sons, New York, 1991, p. 335.
[2] R. Massard, D. Uzio, C. Thomazeau, C. Pichon, J.L. Rousset, J.C. Bertolini, J. Catal. 245 (2007) 133.
[3] M.E. Davis, R.J. Davis, Fundamentals of Chemical Reaction Engineering, 1st ed., McGraw–Hill, New York, 2003.
[4] W. Juszczyk, Z. Karpinski, Appl. Catal. A 206 (2001) 67.
[5] A. Sellidj, B.E. Koel, Phys. Rev. B 49 (12) (1994) 8367.
[6] R.A. Campbell, J.A. Rodriguez, D.W. Goodman, Phys. Rev. B 46 (11) (1992) 7077.
[7] R. Wu, A.J. Freeman, Phys. Rev. B 52 (16) (1995) 12419.
[8] B.E. Koel, A. Sellidj, M.T. Paffett, Phys. Rev. B 46 (12) (1992) 7846.
[9] N.A. Khan, H.H. Hwu, J.G. Chen, J. Catal. 205 (2) (2001) 259.
[10] H.H. Hwu, J.J. Eng, J.G. Chen, J. Am. Chem. Soc. 124 (4) (2002) 702.
[11] G.F. Cabeza, N.J. Castellani, P. Legare, Comput. Mater. Sci. 17 (2000) 255.
[12] V. Pallassana, M. Neurock, G.W. Coulston, J. Phys. Chem. B 103 (1999) 8973.
[13] B. Hammer, J.K. Norskov, Surf. Sci. 343 (1995) 211.
[14] E. Christoffersen, P. Liu, A. Ruban, H.L. Skriver, J.K. Norskov, J. Catal. 199 (2001) 123.
[15] M.B. Zellner, J.G. Chen, J. Catal. 235 (2005) 393.
[16] V. Pallassana, M. Neurock, L.B. Hansen, B. Hammer, J.K. Norskov, Phys. Rev. B 60 (8) (1999) 6146.
[17] V. Pallassana, M. Neurock, J. Catal. 191 (2000) 301.
[18] V. Pallassana, M. Neurock, L.B. Hansen, J.K. Norskov, J. Chem. Phys. 112 (12) (2000) 5435.
[19] S. Alayoglu, A.U. Nilekar, M. Mavrikakis, B. Eichhorn, Nat. Mater. 7 (2008) 333.
[20] F. Epron, F. Gauthard, C. Pineda, J. Barbier, J. Catal. 198 (2001) 309.
[21] F. Gauthard, F. Epron, J. Barbier, J. Catal. 220 (2003) 182.
[22] M.T. Schaal, A.Y. Metcalf, J.H. Montoya, J.P. Wilkinson, C.C. Stork, C.T. Williams, J.R. Monnier, Catal. Today 123 (2007) 142.
[23] M.T. Schaal, A.C. Pickerell, C.T. Williams, J.R. Monnier, J. Catal. 254 (2008) 131.
[24] R.D. Cortright, S.A. Goddard, J.E. Rekoske, J.A. Dumesic, J. Catal. 127 (1991) 342.
[25] J. Okal, L. Kepinski, L. Krajczyk, W. Tylus, J. Catal. 219 (2003) 362.
[26] F. Solymosi, T. Bansagi, J. Phys. Chem. 96 (1992) 1349.
[27] M. Womes, T.C.F.L. Peltier, S. Morin, B. Didillon, Appl. Catal. A 283 (2005) 9.
[28] D. Shen, M. Bulow, F. Siperstein, M. Engelhard, A.L. Meyers, Adsorption 6 (4) (2000) 275.
[29] W. Ranke, Y. Joseph, Phys. Chem. Chem. Phys. 4 (2002) 2483.
[30] S.-C. Chou, S.-H. Lin, C.-T. Yeh, J. Chem. Soc. Faraday Trans. 91 (1995) 949.
[31] K.F. Poulter, J.A. Pryde, J. Phys. D Appl. Phys. 1 (2) (1968) 169.
[32] J. Okal, H. Kubicka, L. Kepinski, L. Krajczyk, Appl. Catal. A 162 (1997) 161.
[33] G.W. Chadzynski, H. Kubicka, Thermochim. Acta 158 (1990) 353.
[34] H. Zea, K. Lester, A.K. Datye, E. Rightor, R. Gulotty, W. Waterman, M. Smith, Appl. Catal. A 282 (2005) 237.
[35] E.W. Hansen, M. Neurock, J. Catal. 196 (2000) 241.
[36] S.A. Goddard, R.D. Cortright, J.A. Dumesic, J. Catal. 137 (1992) 186.
[37] J.E. Rekoske, R.D. Cortright, S.A. Goddard, S.B. Sharma, J.A. Dumesic, J. Phys. Chem. 96 (1992) 1880.
[38] J.G. Chen, C.A. Menning, M.B. Zellner, Surf. Sci. Rep. 63 (2008) 201.
[39] M.P. Humbert, J.G. Chen, J. Catal. 257 (2008) 297.
[40] A.V. Ruban, H.L. Skriver, J.K. Norskov, Phys. Rev. B 59 (24) (1999) 15990.
[41] A. Jablonski, S.H. Overbury, G.A. Samorjai, Surf. Sci. 65 (1977) 578.
[42] S. Zhou, B. Varughese, B. Eichhorn, G. Jackson, K. McIlwrath, Angew. Chem. Int. Ed. 44 (2005) 4539.